Research Article

Patrick Ehi Imoisili, Tien-Chien Jen*, and Babak Safaei*

Microwave-assisted sol–gel synthesis of TiO_2-mixed metal oxide nanocatalyst for degradation of organic pollutant

https://doi.org/10.1515/ntrev-2021-0016
received February 28, 2021; accepted March 19, 2021

Abstract: Titanium dioxide (TiO_2) is the most effective photocatalysts for low-cost degradation of organic pollutant; however, the wide band gap and the high recombination rate of the charge carriers are drawbacks that hinders it practical application. In this study, TiO_2 and titanium mixed metal oxides ternary ($V/Ag/TiO_2$) nanocatalyst was synthesized through a microwave-assisted sol–gel route using Ti $(C_4H_9O)_4$, NH_4VO_3, and $AgNO_3$ as precursors. The XRD analysis of the synthesized TiO_2 and $V/Ag/TiO_2$ depicts lattice fringes for rutile and anatase crystalline phases. Raman spectra indicate the formation of a mesoporous multiphase sample mixture of rutile and anatase phases. The spectrum shift to the visible light region was demonstrated by the UV-visible spectroscopy analysis. Diffuse reflectance spectroscopy (DRS) reveals a reduced band gap of 2.9 eV for TiO_2 and 2.65 eV for $V/Ag/TiO_2$. Brunauer–Emmett–Teller (BET) indicates a large surface area of 92.8 and 84.8 $m^2 g^{-1}$ for TiO_2 and $V/Ag/TiO_2$, respectively. Nitrogen adsorption–desorption isotherm exhibits type IV isotherm, signifying the presence of the mesoporous structure. SEM portrays a cluster of rod-like aggregate particles, while the HRTEM analysis illustrates nanoparticles of rod-like cylindrical shape with a homogeneous size diameter. The synthesized nanocatalyst demonstrated a significant photocatalytic ability in the degradation of methyl orange (MO) and methylene blue (MB). $V/Ag/TiO_2$ shows higher activity in the visible region. Thus, the present report suggests efficient, suitable, and economical microwave-assisted sol–gel techniques to yield $V/Ag/TiO_2$ nanocatalysts with harnessed photocatalytic performance for the degradation of toxic organic pollutants in the presence of visible light irradiation.

Keywords: microwave, mixed metal oxide, nanocatalyst, sol–gel, photocatalysis

1 Introduction

Up till now, a lot of researchers worked on nanostructures, and the use of the nanostructures has been growing rapidly [1]. Nanoscaled adsorbents such as nanofibers, carbon nanotubes, graphene, and metal oxides are extensively employed to improve wastewater and water treatment [2]. Szczepanik *et al.* [3] showed that the photodegradation of aniline and its chloro derivatives shows the existence of Hal-Fe_2O_3. The performance of Hal-TiO_2 nanocomposite is higher than the commercially available photocatalyst P25. Shafey [4] showed that the manufactured biological nanostructures and nanomaterials have a great application in the pharmaceutical industry, such as drug delivery, novel pharmaceuticals preparation, and production of functional nanodevices. The reason for this is that these nanomaterials are assumed to possess better adsorptive performance compared to common adsorbents. Nanosized metal oxides, such as titanium oxide [5] and zinc oxide (ZnO) [6], have shown high adsorption to inorganic and organic pollutant materials. The discovery of photocatalysis has opened up new fields in the world of wastewater treatment [7]. The photocatalysis technology is used as an alternative to environmental protection, detoxification of contaminants, and photodegradation of organic contaminants [8]. The utilization of TiO_2 as a photocatalyst has gained momentum owing to its resistance to photocorrosion [9], chemical stability [10], biological activity [11], and low cost [12]. Still, TiO_2 has three big disadvantages [13]: a high band

* **Corresponding author: Tien-Chien Jen,** Department of Mechanical Engineering Science, University of Johannesburg, Kingsway and University Road, Auckland Park, 2092, P. O. Box 524, Auckland Park, 2006, Johannesburg, South Africa, e-mail: tjen@uj.ac.za
* **Corresponding author: Babak Safaei,** Department of Mechanical Engineering, Eastern Mediterranean University, Famagusta, North Cyprus via Mersin 10, Turkey, e-mail: babak.safaei@emu.edu.tr
Patrick Ehi Imoisili: Department of Mechanical Engineering Science, University of Johannesburg, Kingsway and University Road, Auckland Park, 2092, P. O. Box 524, Auckland Park, 2006, Johannesburg, South Africa

gap value of 3.2 eV; UV-only photocatalytic response with a fast recombination photo-generated pairs of electron–hole; and low photocatalytic reaction quantity in the aqueous phase [14]. Ni *et al.* [15] by considering cold-rolling deformation investigated microhardness and microstructural evolution of two types of electrodeposited gradient nanostructured nickel samples with a symmetric structure.

Titanium dioxide (TiO_2) has been proven to be the most commonly used by different oxide semiconductor photocatalysts [16] because of its good oxidizing strength, long-term photostability, and nontoxicity [17]. Guo *et al.* [18] deposited ultrathin SiO_2 layers by using atomic layer deposition (ALD) on nanoparticles to fabricate core/shell nanostructures. However, the photocatalytic efficiency of TiO_2 to degrade dyes decreases substantially due to the high recombination ratio of photo-induced electrons (e^-) [19] and holes (h^+) produced when irradiated under the ultraviolet (UV) light ($\lambda < 380$ nm) [20]. With nanoscaled external dimensions, TiO_2, a semiconductor photocatalyst, has extensive applications in different industries [21] such as decontamination or mineralization of pollutants in water to harmless inorganic anions [3] and cosmetic materials [22]. Therefore, TiO_2 nanoparticles (T-NPs) have attracted the attention of many researchers because of their extraordinary properties [23]. It is well known that TiO_2 powder in the anatase phase has strong catalytic activity because of its redox properties, surface chemistry, and high surface area. Typek *et al.* [24] studied the magnetic characteristics of several TiO_2/graphitic carbon nanocomposites fabricated at various temperatures (300–850°C) in the presence of benzene vapor. In another study, the effect of hexylamine on the morphology of nano-TiO_2 was investigated by Sun *et al.* [25]. Li *et al.* [26] reviewed theoretical calculations of TiO_2-based commercial photocatalysts in water splitting. Wang *et al.* [27] developed an experimental test method to determine the photocatalytic degradation effect of nano-TiO_2 on oil pollution of road surfaces. Guo *et al.* [28] explored the physicochemical properties of the mixed crystal nano-TiO_2 using the X-ray diffraction (XRD) technique. MgO-modified TiO_2 thin films were characterized using different techniques of instrumental analysis such as SEM-EDS, AFM, XRD, and UV-visible absorption spectrometry. The photoactivity of these structures was also studied using photo-voltammetry followed by splitting water in a twin-cell reactor, where oxygen and hydrogen gases were generated separately [29]. Mahshid *et al.* [30] studied the preparation of titanium oxide with two different polymorphs and reported that the water/titanium molar ratio (r) has been employed to control the hydrolysis and condensation of titanium isopropoxide in solution.

Nanostructures can make a lot of impact on material, and hence, researchers carried out many studies on composites [31] and their photocatalytic activity [32]. In another study, bulk nanocrystalline graphite has been studied for piezoresistive sensors by Simionescu *et al.* [33]. Naghdi *et al.* [34] reviewed different conductive metal nanomaterials and the challenges facing methods of applications and deposition of thin films. Liu *et al.* [35] studied a "cross-relaxation effect" model to investigate the water-induced shape memory effect, relaxation, and strain recovery of amorphous shape memory polymer. Sharma *et al.* [36] shown that the porous Co–Mo–ON alloy nanodendrites supported on nitrogen-doped graphene combines the advantages of oxygen reduction active pyridinic-N or graphitic-N contents and the high kinetic resistance of the graphitic carbon of nitrogen-doped graphene in the acidic medium. To optimize its photocatalytic performance, modification of TiO_2 nanoparticles by noble metals is increasing enormously [37]. The results exerted depend on the noble metal and material chosen, the form of TiO_2 used, the quality of organic dyes, and the medium of photoreaction [38]. Doping modifications, therefore, are perhaps the most popular methods introduced to improve the photocatalytic efficiency of TiO_2 [17]. Therefore, the TiO_2 hybridization with V_2O_5 can expand the absorption spectrum to the area of visible light [39]. It may expand the volume of excitable radiations in the region of visible light, which could as well change the surface and grain morphologies [40], leading to higher absorption of visible light together with an increase in the number of reactive sites that are surface active [41]. But alternatively, deposition of noble metals such as Ag could achieve high absorption within the region of visible light and efficiently isolate the electron–hole pairs attributed to plasmon resonance at the surface [42].

Microwave-assisted sol–gel synthesis is a relatively novel method to produce materials since microwave heating is an in situ mode of energy conversion and is radically different from traditional heating processes [43]. The microwave-assisted sol–gel method has sparked tremendous interest due to its numerous advantages, including the ability to generate small, uniform particles, high crystallinity, regulated morphology, and high purity due to the short reaction time. Microwave treatment has a number of advantages, including ease of use, energy savings, and high yield [44]. Since microwave heating is an in situ mode of energy conversion that is radically different from traditional heating processes, microwave-assisted sol–gel synthesis is a relatively new method of producing materials.

Metal oxide hybridization refers to a technique, whereby for a synergistic effect, two separate semiconductors are

hybridized. In addition to photocatalytic improvement, the noble metal modification allows TiO_2 nanoparticles to be involved in the visible light energy spectrum [45]. The photo-generated electron–hole pairs undertake rotational transport of the two semiconductors, thus lengthening the carrier's lifespan, broadening the absorption spectrum, and using the solar energy. For instance, V_2O_5 is an oxide semiconductor possessing a small band gap of 2.80 eV. Hence, the excellent stability and reproducibility were present in the noble metal-modified TiO_2. Ag^+-modified TiO_2 prepared by Gupta *et al.* [46] was noted to be used in mixed dye (CV and MR) degradation for the second time with 90% effectiveness. Tripathi *et al.* [47] prepared a mixed metal oxides of silver and vanadium-sensitized titanium, using titanium isopropoxide ($C_{12}H_{28}O_4Ti$) as a TiO_2 precursor, vanadium pentoxide (V_2O_5) as a vanadium precursor, and silver chloride (AgCl) as a silver precursor and reported that the metal oxide hybrid catalyst exhibited a superior photocatalytic performance and attributed it to the narrow band gap and reduced electron–hole recombination of the compound. In another study, Zhu *et al.* [39] used tetrabutyl orthotitanate ($C_{16}H_{40}O_4Ti$), as a precursor for titanium, silver nitrate ($AgNO_3$) as silver sources, triisopropoxyvandium (V) oxide ($C_9H_{21}O_4V$) as a precursor for vanadium in synthesizing $Ag/V_2O_5/TiO_2$ ternary nanostructured compound. They systematically studied the relationship between the composition and the morphology of the compound and reported a superior photocatalytic performance of the overneat TiO_2. In one of our recent works, a sol–gel/hydrothermal route was used to prepare a V and Ag mixed-TiO_2 nanocatalyst. We reported enhanced photocatalytic performance and selective degradation of organic pollutants from the river surface water [48]. Improvement of TiO_2 photocatalytic performance with silver and vanadium doping was reported by all previous studies [49].

For this investigation, we aim to synthesized a ternary nanocatalyst and obtain small particles with a narrow size distribution in a short period of reaction time and high purity. Thus, a ternary nanocatalyst using titanium(IV) butoxide [$Ti(C_4H_9O)_4$] as the titanium precursor and, ammonium metavanadate (NH_4VO_3) as the precursor of vanadium, and silver nitrate (Ag_2NO_3) as the silver precursor was synthesized using the microwave-assisted sol–gel method. The microstructural, chemical, photocatalytic, and optical features of the doped photocatalyst were investigated. For evaluation of the photocatalytic performance in degradation of organic pollutant, degradation of methyl orange (MO) and methylene blue (MB) as model pollutant with the use of visible light was examined. This innovation for microwave-assisted sol–gel synthesis of mixed metal hybrid nanocatalyst is for the development of a co-doped TiO_2, with high purity, a short period of reaction time, and small particles with a narrow size distribution. This method will contribute to a faster, simplistic, environmentally friendly, and highly efficient method for the fabrication of high-performance next-generation nanocatalyst.

2 Materials and methods

2.1 Synthesis of materials

To prepare the ternary nanocatalyst, 2 mL titanium(IV) butoxide (97% Sigma-Aldrich) was added dropwise to 50 mL deionized water in a beaker. After 15 min, 5 mL H_2O_2 (35% Sigma-Aldrich), 5 mL $AgNO_3$ (10 mg/L; 99% Sigma-Aldrich), and 5 mL NH_4VO_3 (0.4 mg/L; 99% Sigma-Aldrich) were included in the mixture. Continuous stirring of the yellowish sol mixture was carried out for 15 min. Then, the solution was microwaved with a microwave oven (LG Electronics Model No. MS2596OB) for 2 min at a frequency of 2,450 MHz and 1,000 W. This equipment was programmed at a temperature of 80°C with on–off cycle (20 s on – 40 s off). Unlike conventional heating, the microwave energy directly interacts with the material via molecular interaction with the electromagnetic field, and the material itself generates the heat, which subsequently generates fast homogeneous nucleation and easy gel dissolution. The sample was allowed to cool at room temperature and washed using deionized water and ethanol. The resulting precipitate was dried in oven at 80°C for 2 hours and calcined at 350°C for 1 h [47]. The weight ratio of Ag, V, and TiO_2 was 1:2:6. For the comparative purpose, TiO_2 was also prepared without the addition of vanadium (V) and silver (Ag). This microwave-assisted sol–gel technique is inexpensive, clean, and eco-friendly; reduces energy consumption; fast compared to the conventional sol–gel hydrothermal method. The schematic illustrations of the fabrication procedure are shown in Figure 1.

3 Result and discussion

3.1 Nanocatalyst characterization

The crystal structure was analyzed with XRD using X-Pert Philips at 40 kV acceleration voltage as well as a 40 mA current from 2θ 4° to 75° using powdered samples. The chemical structure was examined by Raman spectroscopy

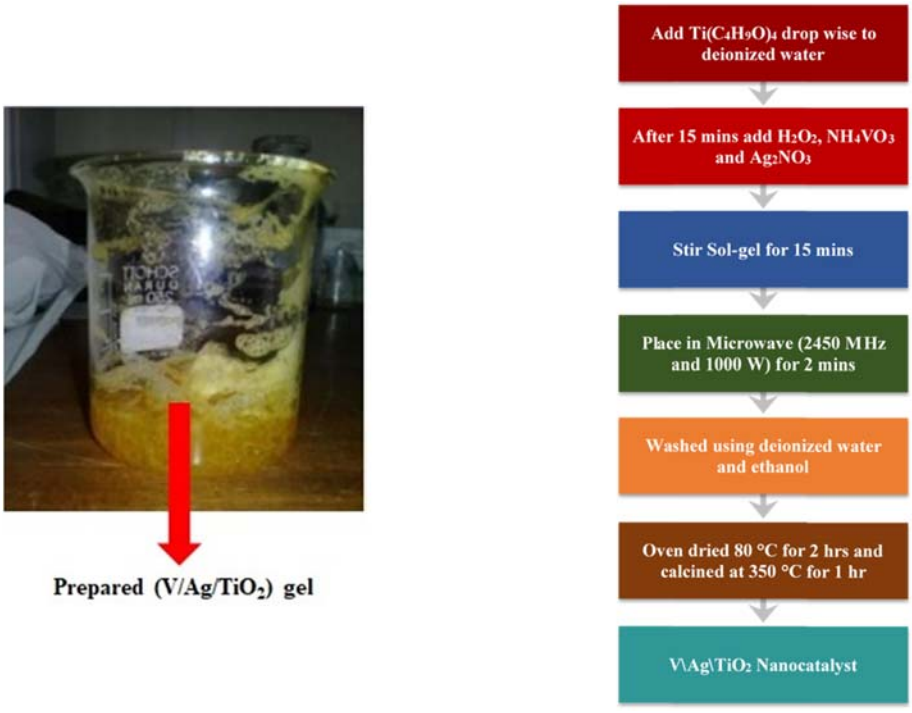

Figure 1: The schematic illustrations and sample preparation for the fabrication procedure.

using a Reinshaw Raman microscope. SEM was carried out using a TESCAN VEGA3. The samples were first place on a carbon substrate in the sample holder, and then sputter coated with car. TEM was performed using a JEM-2100 JEOL electron microscope. The samples for the TEM analysis were first sonicated in ethanol for 5 min, and few drops of the solution were placed on a carbon-coated cropper grid (Sample holder) and used for the analysis. The surface area was studied by Brunauer–Emmett–Teller (BET) using a micrometrics ASAP 2460. UV-Vis analysis was carried out using a UV-Vis-NIR spectra-photometer with a DRA inserter. VG ESCALAB MKII XPS system was employed for the XPS analysis.

3.2 Photocatalytic activity test

In the experiment, MO and MB solutions were prepared and then put to use as a pollutant for the model. A total of 0.2 g of the prepared nanocatalyst was made soluble in 500 mL of 5×10^{-5} MO solution. The MO solution of 10 mg/L of was prepared and used as a model pollutant. A total of 0.2 g of the prepared nanocatalyst was dissolved in 50 mL of the MB solution and then irradiated using a lamp as a visible illumination source ($\lambda = 254$ nm, compact fluorescent integrated lamp 9 W, 50–60 Hz, 220–240 V, Philips, Holland). The solution was stirred mechanically, with exposure to the illumination of visible light. Aliquots of 2 mL were retrieved from the solution and passed through filtration of a PTFE syringe at 30 min time intervals for 3 h. The resultant solution was analyzed by the UV-visible spectrophotometer.

3.3 Photocatalytic evaluation

The supernatant absorbance was determined at 464 nm for MO and 473 nm for MB using applicable blanks. To compare the photocatalytic behavior of the prepared TiO_2 and $V/Ag/TiO_2$ nanocatalyst, the C/Co was plotted as shown in Figure 2. As observed, the synthesized TiO_2 degradation of MO and MB exhibits poor photocatalytic effects with an average removal rate of 72.6% for MO and 73.86% for MB after 60 min compare to $V/Ag/TiO_2$ removal of 98.55% for MO and 99.24% for MB under visible light irradiation. Similar results for TiO_2 degradation of MO and MB have been previously reported [27,38,46]. The improved photocatalytic performance of the $V/Ag/TiO_2$ nanocatalyst can be attributed to an efficient photo-induced structure [46–50]. This structure can be seen as the electron–hole pair separation in the reaction system. The shift of light absorption to the visible region helps in utilizing visible light for the activity of photocatalyst. In addition, the larger surface area contributes to the higher light

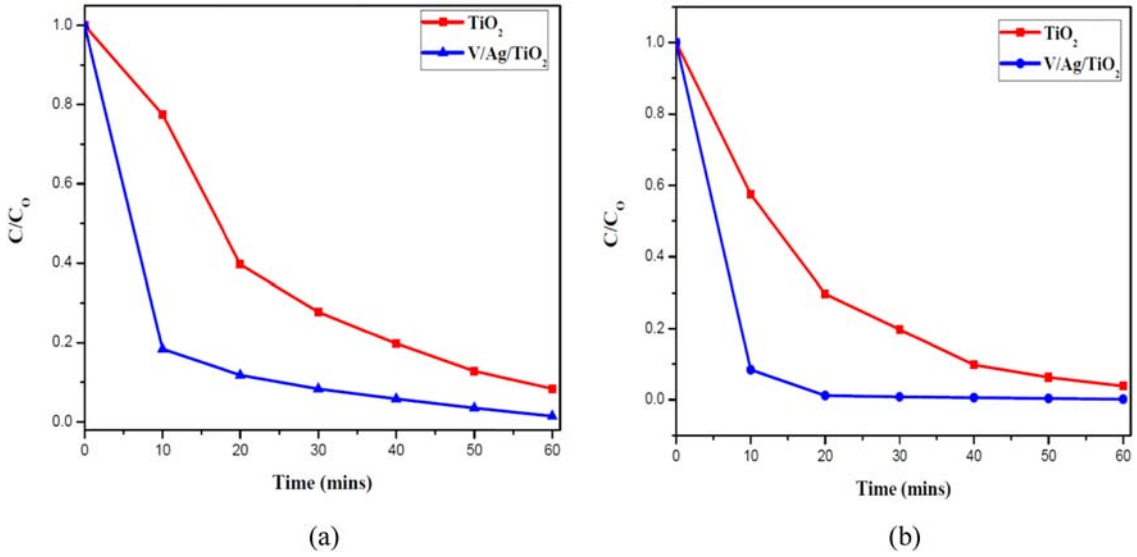

Figure 2: Degradation of (a) methyl orange (b) methylene blue under visible light.

harvesting, which effectively increases the photocatalytic activity of the nanocatalyst.

Figure 3 demonstrates the diffraction phase peaks of TiO_2 and V/Ag/TiO_2. The diffraction peaks reveal the combined crystal phases of both anatase and rutile. The intense peak was observed at a 2θ value of 25.4°. This corresponds to (101) anatase crystal plane for TiO_2 and had consistency with the JCPDS database # 89-4921. Peaks at 37.4°, 42.4°, and 48.2° of (004), (002), and (200) plane are also attributed to the anatase phase of TiO_2 [47]. Peaks at 27.3°, 35.9°, 44.3°, and 55.2° may be attributed to the rutile phase [49]. The addition of the V and Ag dopants resulted in an increase in the anatase phase in the ternary nanocatalyst, and this was in agreement with the previous studies that the addition of dopant increases the anatase phase of TiO_2 [51,52].

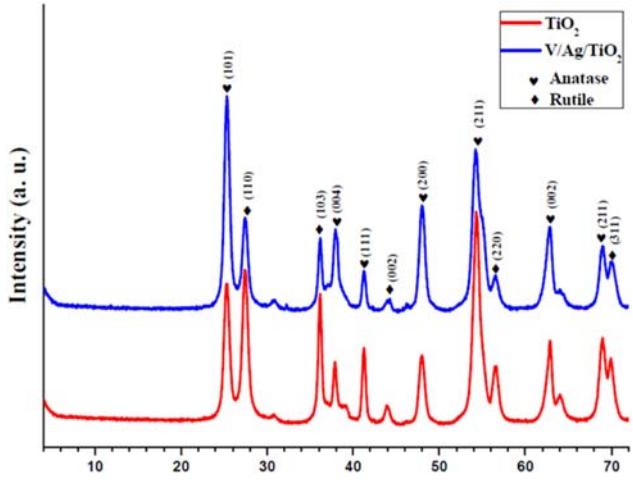

Figure 3: XRD patterns of synthesized TiO_2 and V/Ag/TiO_2 nanostructure photocatalysts.

As shown in Figure 4(a), Raman spectra were measured for further investigation toward the phase structures of distinct samples. Raman bands at 150, 515, and 637 cm^{-1} could be attributed to the crystal phase of anatase, and that of 243, 449, and 615 cm^{-1} were allocated the rutile phase, which indicated the formation of a multiphase mesoporous combined samples of both anatase and rutile crystal phases, indicating consistency with the XRD study [49]. As illustrated in Figure 4(b), in comparison to the prepared TiO_2 sample, the major band at 150 cm^{-1} for V/Ag/TiO_2 was widened and then slightly shifted, which can be attributed to the disorganization of the TiO_2 crystals, which resulted from the effects of the phonon confinement or the crystal size [53–55].

S_{BET} results for TiO_2 and V-Ag/TiO_2, were 104.8 and 122.8 $m^2\,g^{-1}$, respectively. Also, V/Ag/TiO_2 nanocatalyst possesses the higher surface area due to the miniature crystallite sizes of the sample. It has been reported from the previous research that with higher specific surface areas, there is an increase in photocatalyst activities since it provides additional sites for the absorption of light. As such, the high surface area of the synthesized nanocrystal contributed to the effective degradation of MO and MB [48,50,56]. Figure 5 displays the nitrogen adsorption–desorption isotherm, which exhibits a type IV isotherm, indicating the existence of the mesoporous structure in association with the absorbent capillary condensation [57]. Figure 6 shows the pore size distribution

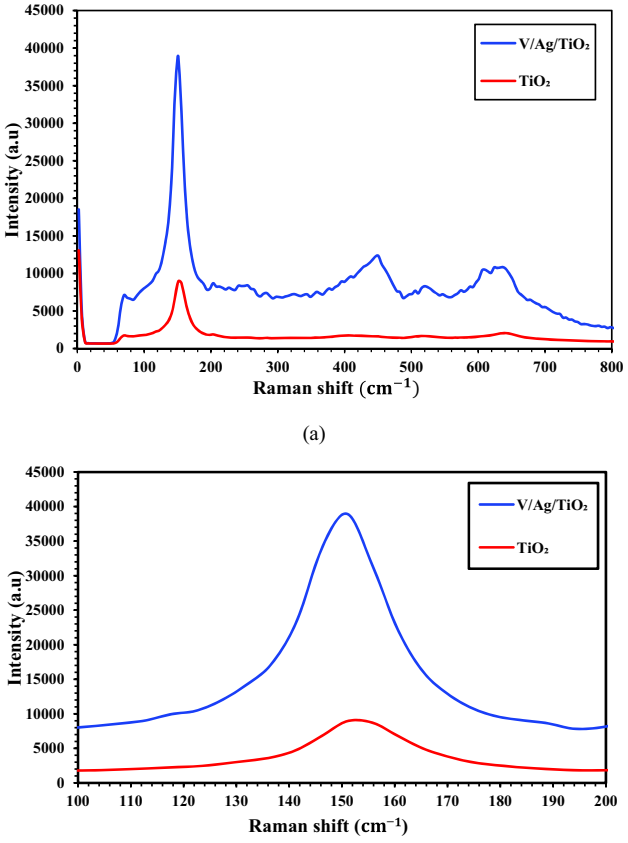

Figure 4: Raman spectral of synthesized TiO_2 and V/Ag/TiO_2 nanostructure photocatalysts.

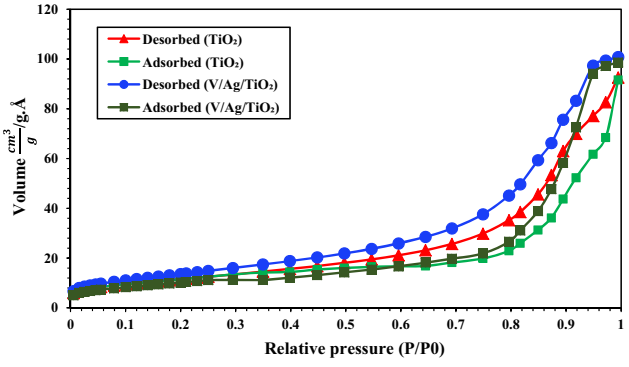

Figure 5: The nitrogen adsorption–desorption isotherms of the synthesized TiO_2 and V/Ag/TiO_2.

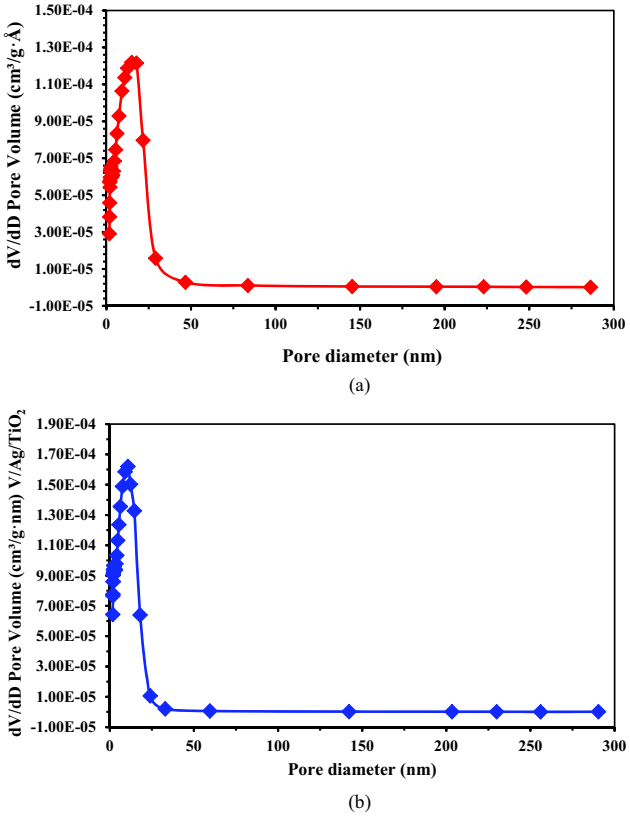

Figure 6: Pore size distribution of the synthesized (a) TiO_2 and (b) V/Ag/TiO_2.

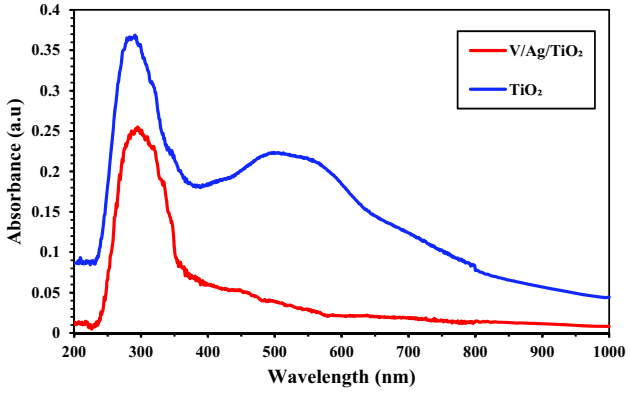

Figure 7: Absorbance spectrum of the synthesized TiO_2 and V/Ag/TiO_2.

of the synthesized (a) TiO_2 and (b) V/Ag/TiO_2. There was a minimal distribution of the mesoporous pores of uniform sizes ranging from 2 to 28 nm.

Figure 7 demonstrates the spectrum absorbance of the synthesized nanocatalyst. The absorption edges of TiO_2 were observed at 404 nm and was similar to the previous studies by Khutso *et al.* [49] and Liu *et al.* [58]. Doping of TiO_2 with silver and vanadium shows a remarkable increase in photocatalytic activities at the irradiation of visible light [47]. Emphasizing the synergistic impact of vanadium and silver, their influence has brought about an increased kinetic reaction as a result of moving the light absorption toward the region of visible

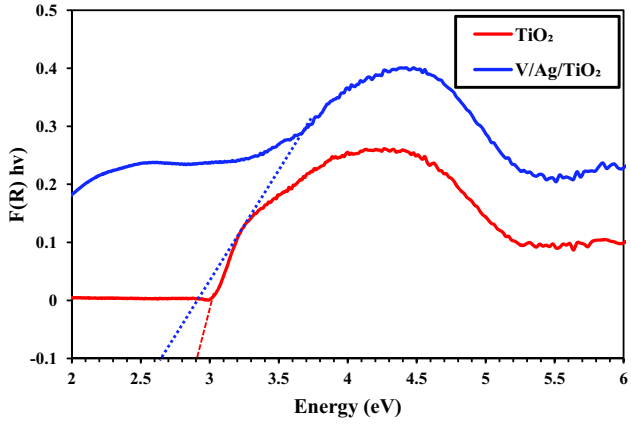

Figure 8: Energy band gap of the synthesized TiO_2 and $V/Ag/TiO_2$.

light, hence gathering increased energy quantity. $V/Ag/TiO_2$ absorption edge moved to the increased wavelength with an added peak around the shoulder close to 580 nm. This suggested that the $V/Ag/TiO_2$ nanocatalyst can be successfully utilized in the visible light spectrum [47,49]. The doping effects of V and Ag significantly improve the light absorption at extended wavelengths (>400 nm) which is in the existence of the visible light regions [49]. The calculation of the energy band gap (eV) was employed for the evaluation of the energy needed for activating the nanocatalyst. Each nanocatalyst's energy band gap (eV) was determined using the Tauc equation [59]. As illustrated in Figure 8, the band gap energies of TiO_2 and $V/Ag/TiO_2$ were interpolated to be 2.9, and 2.65 eV, respectively. The nanocatalyst $V/Ag/TiO_2$ has achieved the desired minimal band energy value. The reduced band gap allows

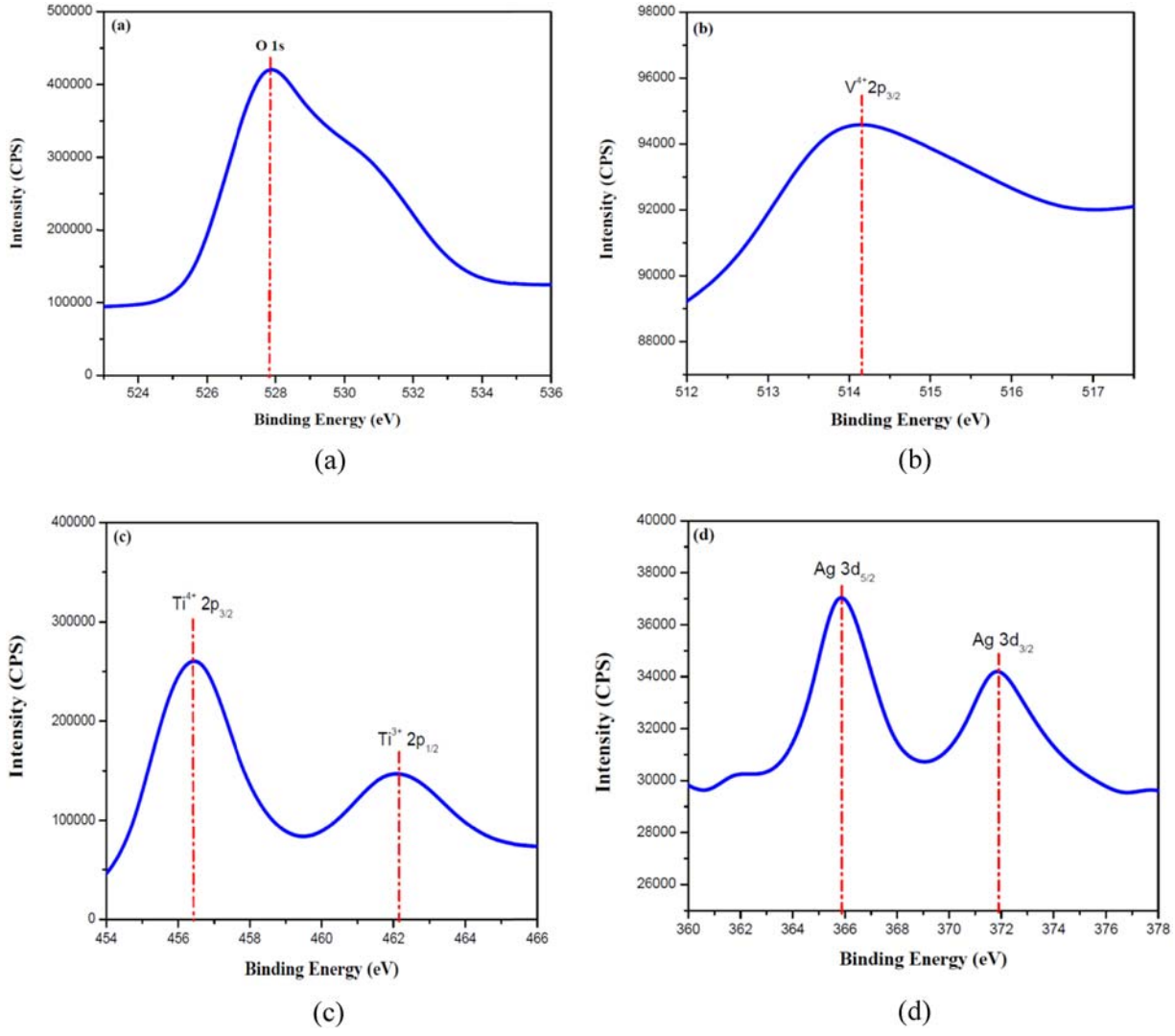

Figure 9: XPS spectra of (a) O 1s, (b) V 2p, (c) Ti 2p, and (d) Ag 3d of the synthesized $V/Ag/TiO_2$.

activation of the nanocatalyst with lower energy within the visible light region.

The XPS examination (Figure 9) reveals binding states of oxygen in the synthesized V/Ag/TiO_2 nanocatalyst sample. O 1s spectral was observed at a 527.8 eV binding energy, which could be allotted to oxygen lattice in TiO_2 [55]. V $2p_{3/2}$ binding energy was observed at a peak value of 514.1 eV, demonstrating the existence of V^{3+} at the surface of the catalyst in the IV state [48,58]. Binding energy peaks of Ti $2p_{1/2}$ and Ti $2p_{3/2}$ occur at 462.3 and 456.75 eV, respectively, indicating the formation of Ti^{4+} and Ti^{3+} in TiO_2, and these results were similar to that obtained by other researchers [55,57]. Low binding energies of Ag $3d_{3/2}$ and Ag $3d_{5/2}$ were observed at 371. 90 and 365.85 eV, respectively [60].

As shown in Figure 10(a), the SEM image for V/Ag/TiO_2 describes the creation of a closely stacked cluster

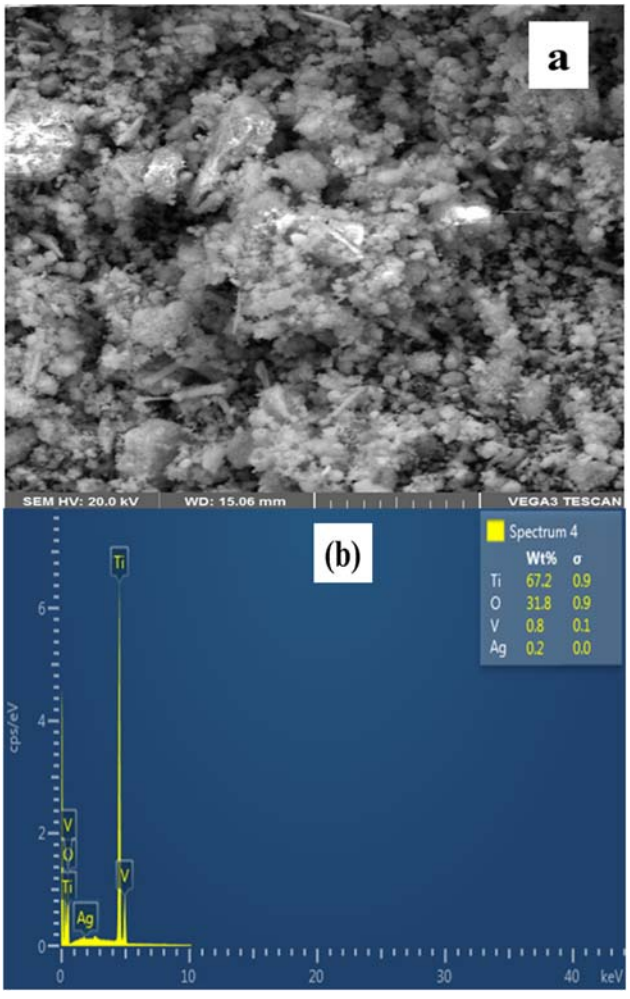

Figure 10: Morphology of V/Ag/TiO_2 nanocatalyst: (a) SEM image (b) EDX mapping.

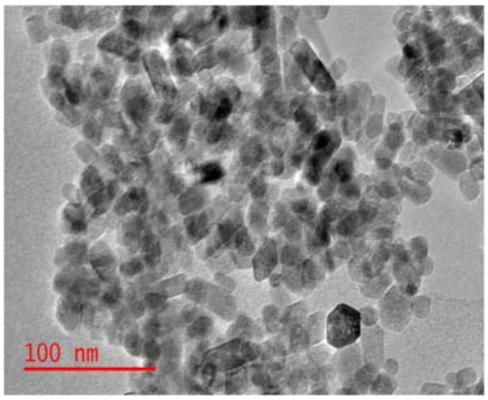

Figure 11: HRTEM images of V/Ag/TiO_2.

comprising rod-like aggregated particles of diameters of nonuniform sizes, while Figure 10(b) displays the EDX mapping showing the composition of the nanocatalyst. HRTEM images for the prepared nanocatalyst are shown in Figure 11. The synthesized V/Ag/TiO_2 nanocatalyst was rod-like cylinder with a homogeneous size diameter ranging between 15 and 45 nm. This rod-like shape can be attributed to the type of synthesis method and precursor employed as this differs from the rectangular shape reported by Zhu *et al.* [39]. The photocatalyst with a rod-like shape has been reported to be very effective in organic dye degradation [49].

4 Conclusion

Vanadium and silver co-doped titanium oxide ternary nanocatalyst was successfully synthesized using a microwave-assisted sol–gel method. The co-doped photocatalyst shows the reduced band gap of 2.65 eV, the large surface area of 84.8 $m^2 g^{-1}$, and the particle size between 15 and 45 nm. The synthesized V/Ag/TiO_2 demonstrated the ability of these photocatalysts in successfull degradation of MO and MB, indicating the prevention of recombination of the electron hole. The synthesis of a microwave-assisted sol–gel ternary nanocatalyst is easier and faster, and nanoparticles with a larger surface area are produced. Generally, this article presents a framework for the development of microwave-assisted sol–gel synthesis of a co-doped TiO_2, with high purity, a short period of reaction time, and small particles with a narrow size distribution. This method is facile, environmentally friendly, and highly efficient for the fabrication of high-performance next-generation nanocatalyst.

Funding information: The authors would like to appreciate the funding from URC of University of Johannesburg. T. C. Jen would like to acknowledge the financial support from NRF, as well.

Author contributions: All authors have accepted responsibility for the entire content of this manuscript and approved its submission.

Conflict of interest: The authors state no conflict of interest.

References

[1] Wu Q, Miao WS, Zhang YD, Gao HJ, Hui D. Mechanical properties of nanomaterials: a review. Nanotechnol Rev. 2020;9:259–73. doi: 10.1515/ntrev-2020-0021.

[2] Nasirian M, Mehrvar M. Modification of TiO_2 to enhance photocatalytic degradation of organics in aqueous solutions. J Environ Chem Eng. 2016;4:4072–82. doi: 10.1016/j.jece.2016.08.008.

[3] Szczepanik B, Rogala P, Słomkiewicz PM, Banaś D, Kubala-Kukuś A, Stabrawa I. Synthesis, characterization and photocatalytic activity of TiO_2-halloysite and Fe_2O_3-halloysite nanocomposites for photodegradation of chloroanilines in water. Appl Clay Sci. 2017;149:118–26. doi: 10.1016/j.clay.2017.08.016.

[4] Shafey AMEL. Green synthesis of metal and metal oxide nanoparticles from plant leaf extracts and their applications: a review. Green Process Synth. 2020;9:304–39. doi: 10.1515/gps-2020-0031.

[5] Syngouna VI, Chrysikopoulos CV, Kokkinos P, Tselepi MA, Vantarakis A. Cotransport of human adenoviruses with clay colloids and TiO_2 nanoparticles in saturated porous media: effect of flow velocity. Sci Total Environ. 2017;598:160–7. doi: 10.1016/j.scitotenv.2017.04.082.

[6] Chouchene B, Chaabane TBen, Mozet K, Girot E, Corbel S, Balan L, et al. Porous Al-doped ZnO rods with selective adsorption properties. Appl Surf Sci. 2017;409:102. doi: 10. 10.1016/j.apsusc.2017.03.018.

[7] Mustapha S, Ndamitso MM, Abdulkareem AS, Tijani JO, Shuaib DT, Ajala AO, et al. Application of TiO_2 and ZnO nanoparticles immobilized on clay in wastewater treatment: a review. Appl Water Sci. 2020;10:49. doi: 10.1007/s13201-019-1138-y.

[8] Pawar M, Sendoğdular ST, Gouma P. A brief overview of TiO_2 photocatalyst for organic dye remediation: case study of reaction mechanisms involved in Ce–TiO_2 photocatalysts system. J Nanomater. 2018:2018. doi: 10.1155/2018/5953609.

[9] Ramesh S, Devred F, Debecker DP. $NaAlO_2$ supported on titanium dioxide as solid base catalyst for the carboxymethylation of allyl alcohol with DMC. Appl Catal A Gen. 2019;581:31–6. doi: 10.1016/j.apcata.2019.05.017.

[10] Sun X, Sun B, Gong Q, Gao T, Zhou G. Double-shell structural polyaniline-derived TiO_2 hollow spheres for enhanced photocatalytic activity. Transit Met Chem. 2019;44(555–64):8. doi: 10.1007/s11243-019-00312.

[11] Bourezgui A, Kacem I, Daoudi M, Al-Hossainy AF. Influence of gamma-irradiation on structural, optical and photocatalytic performance of TiO_2 nanoparticles under controlled atmospheres. J Electron Mater. 2020;49:1904–21. doi: 10.1007/s11664-019-07887-z.

[12] Li C, Zhu N, Dong X, Zhang X, Chen T, Zheng S, et al. Tuning and controlling photocatalytic performance of TiO_2/kaolinite composite towards ciprofloxacin: role of 0D/2D structural assembly. Adv Powder Technol. 2020;31:1241–52. doi: 10.1016/j.apt.2020.01.007.

[13] Al Zoubi W, Salih Al-Hamdani AA, Sunghun B, Ko YG. A review on TiO_2-based composites for superior photocatalytic activity. Rev Inorg Chem. 2021. doi: 10.1515/revic-2020-0025.

[14] Bakbolat B, Daulbayev C, Sultanov F, Beissenov R, Umirzakov A, Mereke A, et al. Recent developments of TiO_2-based photocatalysis in the hydrogen evolution and photodegradation: a review. Nanomaterials. 2020;10:1790. doi: 10.3390/nano10091790.

[15] Ni H, Wang L, Wang Z, Zhu J. Grain orientation induced softening in electrodeposited gradient nanostructured nickel during cold rolling deformation. Rev Adv Mater Sci. 2020;59:144–50. doi: 10.1515/rams-2020-0105.

[16] Yan Z, He Z, Li M, Zhang L, Luo Y, He J, et al. Curcumin doped SiO_2/TiO_2 nanocomposites for enhanced photocatalytic reduction of Cr(VI) under visible light. Catalysts. 2020;10:942. doi: 10.3390/catal10080942.

[17] Shi W, Duan D, Wang H, Ma C, Sun Z, Song X. Improving the photocatalytic performance of a sea-cucumber-like nanoporous TiO_2 loaded with Pt[sbnd]Ag for water splitting. Int J Hydrogen Energy. 2019;44:13040–51. doi: 10.1016/j.ijhydene.2019.03.196.

[18] Guo J, Benz D, Doan Nguyen TT, Nguyen PH, Thi Le TL, Nguyen HH, et al. Tuning the photocatalytic activity of TiO_2 nanoparticles by ultrathin SiO_2 films grown by low-temperature atmospheric pressure atomic layer deposition. Appl Surf Sci. 2020;530:147244. doi: 10.1016/j.apsusc.2020.147244.

[19] Ariyanti D, Maillot M, Gao W. TiO_2 used as photocatalyst for rhodamine B degradation under solar radiation. Int J Mod Phys B (World Scientific Publishing Co. Pte Ltd). 2017;31:16–9. doi: 10.1142/S0217979217440957.

[20] Allen NS, Vishnyakov V, Kelly PJ, Kriek RJ, Mahdjoub N, Hill C. Characterisation and photocatalytic assessment of TiO_2 nanopolymorphs: Influence of crystallite size and influence of thermal treatment on paint coatings and dye fading kinetics. J Phys Chem Solids. 2019;126:131–42. doi: 10.1016/j.jpcs.2018.11.004.

[21] Bayal N, Jeevanandam P. Synthesis of TiO_2–MgO mixed metal oxide nanoparticles via a sol–gel method and studies on their optical properties. Ceram Int. 2014;40:15463–77. doi: 10.1016/j.ceramint.2014.06.122.

[22] Ghafoori S, Nasirian M, Al-Jamal R, Mallouh FA, Mehrvar M. Statistical parameter optimization and modeling of photodegradation of methyl orange using a composite photocatalyst prepared by thermal synthesis. Environ Sci Pollut Res. 2020;27:45650–60. doi: 10.1007/s11356-020-10301-5.

[23] Dariani RS, Esmaeili A, Mortezaali A, Dehghanpour S. Photocatalytic reaction and degradation of methylene blue on TiO_2 nano-sized particles. Optik (Stuttg). 2016;127:7143–54. doi: 10.1016/j.ijleo.2016.04.026.

[24] Typek J, Guskos N, Zolnierkiewicz G, Pilarska M, Guskos A, Kusiak-Nejman E, et al. Magnetic properties of TiO_2/graphitic carbon nanocomposites. Rev Adv Mater Sci. 2019;58:107–22. doi: 10.1515/rams-2019-0009.
[25] Sun P, Wang S, Li Y, Zhang T, Wang D, Zhang B, et al. One-pot synthesis of nano titanium dioxide in supercritical water. Nanotechnol Rev. 2020;9:410–7. doi: 10.1515/ntrev-2020-0030.
[26] Li B, Wu S, Gao X. Theoretical calculation of a TiO_2-based photocatalyst in the field of water splitting: a review. Nanotechnol Rev. 2020;9:1080–103. doi: 10.1515/ntrev-2020-0085.
[27] Wang Q, Zheng K, Yu H, Zhao L, Zhu X, Zhang J. Laboratory experiment on the nano-TiO_2 photocatalytic degradation effect of road surface oil pollution. Nanotechnol Rev. 2020;9:922–33. doi: 10.1515/ntrev-2020-0072.
[28] Guo Z, Huang C, Chen Y. Experimental study on photocatalytic degradation efficiency of mixed crystal nano-TiO_2 concrete. Nanotechnol Rev. 2020;9:219–29. doi: 10.1515/ntrev-2020-0019.
[29] Huang CW, Liao CH, Wu JCS. Photocatalytic water splitting using hygroscopic MgO modified TiO_2/WO3 dual-layer photocatalysts. Korean J Chem Eng. 2020;37:1352–9. doi: 10.1007/s11814-020-0603-5.
[30] Mahshid S, Askari M, Sasani Ghamsari M, Afshar N, Lahuti S. Mixed-phase TiO_2 nanoparticles preparation usingsol–gel method. J Alloy Compd. 2009;478:586. doi: http://dx.doi.org/10.1016/j.jallcom.2008.11.094.
[31] Tomar SS, Zafar S, Talha M, Gao W, Hui D. State of the art of composite structures in non-deterministic framework: a review. Thin-Walled Struct. 2018;132:700–16. doi: 10.1016/j.tws.2018.09.016.
[32] Aman N, Satapathy PK, Mishra T, Mahato M, Das NN. Synthesis and photocatalytic activity of mesoporous cerium doped TiO_2 as visible light sensitive photocatalyst. Mater Res Bull. 2012;47:179–83. doi: 10.1016/j.materresbull.2011.11.049.
[33] Simionescu OG, Pachiu C, Ionescu O, Dumbravescu N, Buiu O, Popa RC, et al. Nanocrystalline graphite thin layers for low-strain, high-sensitivity piezoresistive sensing. Rev Adv Mater Sci. 2020;59:306–13. doi: 10.1515/rams-2020-0031.
[34] Naghdi S, Rhee K, Hui D, Park S. A review of conductive metal nanomaterials as conductive, transparent, and flexible coatings, thin films, and conductive fillers: different deposition methods and applications. Coatings. 2018;8:278. doi: 10.3390/coatings8080278.
[35] Liu C, Lu H, Li G, Hui D, Fu YQA. "cross-relaxation effects" model for dynamic exchange of water in amorphous polymer with thermochemical shape memory effect. J Phys D Appl Phys. 2019;52:345305. doi: 10.1088/1361-6463/ab2860.
[36] Sharma K, Hui D, Kim NH, Lee JH. Facile synthesis of N-doped graphene supported porous cobalt molybdenum oxynitride nanodendrites for the oxygen reduction reaction. Nanoscale. 2019;11:1205–16. doi: 10.1039/c8nr06780e.
[37] Basavarajappa PS, Patil SB, Ganganagappa N, Reddy KR, Raghu AV, Reddy CV. Recent progress in metal-doped TiO_2, non-metal doped/codoped TiO_2 and TiO_2 nanostructured hybrids for enhanced photocatalysis. Int J Hydrogen Energy. 2020;45:7764–78. doi: 10.1016/j.ijhydene.2019.07.241.
[38] Feizpoor S, Habibi-Yangjeh A. Ternary $TiO_2/Fe_3O_4/CoWO_4$ nanocomposites: novel magnetic visible-light-driven photocatalysts with substantially enhanced activity through p-n heterojunction. J Colloid Interface Sci. 2018;524:325–36. doi: 10.1016/j.jcis.2018.03.069.
[39] Zhu XD, Zheng YL, Feng YJ, Sun KN. Delicate $Ag/V_2O_5/TiO_2$ ternary nanostructures as a high-performance photocatalyst. J Solid State Chem. 2018;258:691–4. doi: 10.1016/j.jssc.2017.12.001.
[40] Hwang SH, Kim C, Jang J. SnO_2 nanoparticle embedded TiO_2 nanofibers – Highly efficient photocatalyst for the degradation of rhodamine B. Catal Commun. 2011;12:1037–41. doi: 10.1016/j.catcom.2011.02.024.
[41] Shi W, Ma C, Wang H, Duan D, Sun Z, Yang S. A sea cucumber-like nanoporous TiO_2 modified by bimetal Pt–Au through the dealloying for water splitting. Int J Hydrogen Energy. 2018;43:18850–62. doi: 10.1016/j.ijhydene.2018.08.180.
[42] Bumajdad A, Madkour M. Understanding the superior photocatalytic activity of noble metals modified titania under UV and visible light irradiation. Phys Chem Chem Phys. 2014;16:7146–58. doi: 10.1039/c3cp54411g.
[43] Rahimi N, Pax RA, Gray EMA. Review of functional titanium oxides. I: TiO_2 and its modifications. Prog Solid State Chem. 2016;44:86–105. doi: 10.1016/j.progsolidstchem.2016.07.002.
[44] Wang Z, Zhu J, Xu W, Sui J, Peng H, Tang X. Microwave hydrothermal synthesis of perovskite $BiFeO_3$ nanoparticles: an insight into the phase purity during the microwave heating process. Mater Chem Phys. 2012;135:330–3. doi: 10.1016/j.matchemphys.2012.04.053.
[45] Kadam AN, Dhabbe RS, Kokate MR, Gaikwad YB, Garadkar KM. Preparation of N doped TiO_2 via microwave-assisted method and its photocatalytic activity for degradation of Malathion. Spectrochim Acta A. 2014;133:669–76. doi: 10.1016/j.saa.2014.06.020.
[46] Gupta AK, Pal A, Sahoo C. Photocatalytic degradation of a mixture of crystal violet (basic violet 3) and methyl red dye in aqueous suspensions using Ag^+ doped TiO_2. Dye Pigment. 2006;69:224–32. doi: 10.1016/j.dyepig.2005.04.001.
[47] Tripathi AM, Nair RG, Samdarshi SK. Visible active silver sensitized vanadium titanium mixed metal oxide photocatalyst nanoparticles through sol–gel technique. Sol Energy Mater Sol Cells. 2010;94:2379–85. doi: 10.1016/j.solmat.2010.08.022.
[48] Ntobeng MK, Imoisili PE, Jen TC. Facile fabrication of vanadium sensitized silver titanium oxides (V–Ag/TiO_2) photocatalyst nanocomposite for pollutants removal in river water. Mater Sci Semicond Process. 2021;123:105569. doi: 10.1016/j.mssp.2020.105569.
[49] Khutso Ntobeng M, Ehi Imoisili P, Jen TC. Synthesis and photocatalytic performance of Ag-$TiVO_X$ nanocomposite. J King Saud Univ Sci. 2020;32:3103. doi: 10. 10.1016/j.jksus.2020.08.021.
[50] Liu G, Qin J, Zhou Z, Liu C, Li F, Wu W. Mesoporous V-TiO_2 catalysts with crystalline anatase-rutile mixed phases for naphthalene degradation. ChemistrySelect. 2019;4:12955–62. doi: 10.1002/slct.201902487.
[51] Ren J, Wang W, Sun S, Zhang L, Chang J. Enhanced photocatalytic activity of Bi_2WO_6 loaded with Ag nanoparticles under visible light irradiation. Appl Catal B Environ. 2009;92:50–5. doi: 10.1016/j.apcatb.2009.07.022.
[52] Sangpour P, Hashemi F, Moshfegh AZ. Photoenhanced degradation of methylene blue on cosputtered M:TiO_2 (M = Au, Ag, Cu) nanocomposite systems: A comparative

study. J Phys Chem C. 2010;114:13955–61. doi: 10.1021/jp910454r.

[53] Saito K, Tominaka S, Yoshihara S, Ohara K, Sugahara Y, Ide Y. Room-temperature rutile TiO_2 nanoparticle formation on protonated layered titanate for high-performance heterojunction creation. ACS Appl Mater Interfaces. 2017;9:24538–44. doi: 10.1021/acsami.7b04051.

[54] Leshuk T, Parviz R, Everett P, Krishnakumar H, Varin RA, Gu F. Photocatalytic activity of hydrogenated TiO_2. ACS Appl Mater Interfaces. 2013;5:1892–5. doi: 10.1021/am302903n.

[55] Chen S, Li D, Liu Y, Huang W. Morphology-dependent defect structures and photocatalytic performance of hydrogenated anatase TiO_2 nanocrystals. J Catal. 2016;341:126–35. doi: 10.1016/j.jcat.2016.06.016.

[56] Reddy BM, Chowdhury B, Ganesh I, Reddy EP, Rojas TC, Fernández A. Characterization of V_2O_5/TiO_2-ZrO_2 catalysts by XPS and other techniques. J Phys Chem B. 1998;102:10176–82. doi: 10.1021/jp9826165.

[57] Dolgonos A, Mason TO, Poeppelmeier KR. Direct optical band gap measurement in polycrystalline semiconductors: a critical look at the tauc method. J Solid State Chem. 2016;240:43–8. doi: 10.1016/j.jssc.2016.05.010.

[58] Liu J, Han R, Zhao Y, Wang H, Lu W, Yu T, et al. Enhanced photoactivity of V–N codoped TiO_2 derived from a two-step hydrothermal procedure for the degradation of PCP-Na under visible light irradiation. J Phys Chem C. 2011;115:4507–15. doi: 10.1021/jp110814b.

[59] Xiang Q, Yu J, Wang W, Jaroniec M. Nitrogen self-doped nanosized TiO_2 sheets with exposed {001} facets for enhanced visible-light photocatalytic activity. Chem Commun. 2011;47:6906–8. doi: 10.1039/c1cc11740h.

[60] Zhang H, Wang G, Chen D, Lv X, Li J. Tuning photoelectrochemical performances of Ag–TiO_2 nanocomposites via reduction/oxidation of Ag. Chem Mater. 2008;20:6543–9. doi: 10.1021/cm801796q.